Contrib. Plasma Phys. **51**, No. 5, 444 – 450 (2011) / **DOI** 10.1002/ctpp.201110015

Optimization of Laser-Generated Ion Beams

S. Steinke[*1], **M. Schnürer**[1], **T. Sokollik**[1,2,3], **A. A. Andreev**[1,4], **P. V. Nickles**[5], **A. Henig**[6,7], **R. Hörlein**[6,7], **D. Kiefer**[6,7], **D. Jung**[7,8], **J. Schreiber**[6,7], **T. Tajima**[6,7,9], **M. Hegelich**[8], **D. Habs**[6,7], and **W. Sandner**[1,10]

[1] Max-Born-Institut, Max-Born-Str. 2A, D-12489 Berlin, Germany
[2] Lawrence Berkeley National Laboratory, 1 Cyclotron Road, Berkeley, California 94720, USA
[3] University of California, Berkeley, California 94720, USA
[4] STC Vavilov State Optical Institute, 12 Birzhevaya line, 199034 St. Petersburg, Russia
[5] Gwangju Institute of Science and Technology, GIST, Gwangju 500-712, Republic of Korea
[6] Max-Planck-Institut für Quantenoptik, Hans-Kopfermann-Str. 1, D-85748 Garching, Germany
[7] Department für Physik, Ludwig-Maximilians-Universität München, D-85748 Garching, Germany
[8] Los Alamos National Laboratory, Los Alamos, New Mexico 87545, USA
[9] Photomedical Research Center, JAEA, Kyoto, Japan
[10] Technische Universität Berlin, Strasse des 17. Juni 135, D-10623 Berlin, Germany

Received 14 April 2010, accepted 23 December 2010
Published online 06 June 2011

Key words Laser-driven acceleration, Laser-plasma interactions, Laser-produced plasma.

In this paper the route towards the current optimum of laser generated ion beams by subsequently changing the important parameters such as target thickness, laser pulse contrast, angle of incidence and laser pulse polarization is sketched. Beginning with parameters of isothermal target normal sheath acceleration (TNSA), we reached the regime where the plasma expansion can be described adiabatically and results in a symmetric ion acceleration. Further we demonstrated a way to phase match the accelerating electron population with the ions, namely coherent acceleration of ions by laser pulses (CAIL), which finally lead to radiation pressure acceleration (RPA) if the laser polarization was changed from linear to circular. These findings of ion acceleration with transparent solid targets are additionally supported by analyzing the optical properties of the transmitted laser pulse.

1 Introduction

Recent experiments have shown that the maximum energy and the number of ions generated by the interaction of a high-intensity laser pulses with solid targets can be improved significantly if targets with thicknesses below the collisionless skin depth of the laser, i. e. partly transparent targets are employed [1]. In contrast to experiments carried out in the parameter range of TNSA [2, 3], where the laser energy is inefficiently transferred to electrons of an underdense plasma at the target front side and most of the laser pulse is reflected, the experiments in the transparent regime enable the participation of the whole focal volume in the acceleration. Moreover, the group velocities of photons, electrons and subsequently that of the ions are matched which manifests in the coherence of the electron motion with respect to the laser field [4,5]. Specifically, this scenario leads in case of circular laser polarization to a dominant RPA, which has attracted a lot of theoretical interest during the last years [6–14] and has recently been demonstrated experimentally [15].

In this report, we sketch the route towards this optimum of laser-ion acceleration. To reach the transparency regime in the first place, technical requirements such as intense laser pulses with an ultra-high temporal contrast and freestanding foil targets with thicknesses of a few nanometers have to be provided. The transition from conventional TNSA to the transparency regime is presented stepwise, beginning with a typical situation for TNSA: a laser pulse with a moderate contrast ratio, obliquely incident on a thick foil target. Then successively the influences of angle of incidence, contrast ratio and target thickness are characterized by means of ion spectra.

* Corresponding author: E-mail: steinke@mbi-berlin.de, Phone: +49 30 6392 1318, Fax: +49 30 6392 1329

Once the foils get transparent for the relativistic laser pulses, the optical properties of the transmitted laser pulse are analyzed in terms of transmittance and spectral shape.

2 Experiment

The experiments were performed at the MBI multi-ten-TW Ti:Sapphire laser delivering 1.2 J in 45 fs FWHM pulses at a central wavelength of 810 nm with an intrinsic amplified spontaneous emission (ASE) contrast ratio better than 10^{-7} up to $\sim$ 10 ps prior to the arrival of the main pulse. By means of a re-collimating Double-Plasma-Mirror (DPM) [16], this contrast can be increased to an estimated value of 10^{11} (UHC) [17], which is essential for the suppression of pre-heating and expansion due to the pulse background. The energy throughput of this DPM system was on the order of 60-65 %, resulting in pulse energies of 0.7 J. Finally, the laser pulse was focused on targets (Diamond-Like-Carbon (DLC) or Titanium (Ti)) with a f/2.5 parabolic mirror down to a diameter of 3.6 μm and therefore a peak intensity of 5×10^{19} W/cm^2, i. e. $a_0 = 5$ or correspondingly, in case of oblique incidence $a_0 = 3.6$ was reached. The resulting ions were detected in target normal direction with two Thomson-Parabolas [18], detecting the ions emerging from the target front (laser illuminated) and rear side. The target can be rotated to change the angle of incidence from oblique ($45°$) to normal. In case of normal incidence, a third ion spectrometer is placed in laser propagation direction. Additionally, the transmitted laser pulse was registered with a 12-bit optical grating spectrometer.

Besides commercially available Ti-foil targets with a thickness of 5 μm, DLC targets of thicknesses ranging from $2.9 - 50$ nm were used, having a density of 2.7 g/cm^3. Owing to the high fraction of sp^3-, i.e. diamond-like bonds of $\sim$75%, DLC offers unique properties for the production of mechanically stable, ultra-thin, free standing targets, such as exceptionally high tensile strength, hardness and heat resistance. The thickness of the DLC foils was characterized by means of an atomic force microscope (AFM), including the hydrocarbon contamination layer on the target surface which was present during the experiments [5]. In order to precisely determine the structure of the contamination layer, the depth-dependent composition of the foil was measured via Elastic Recoil Detection Analysis (ERDA). From these measurements we obtain a thickness of $\sim$ 1 nm of the hydrocarbon contamination layer. In the following the combined thickness of bulk and surface layer as it appears in the actual ion acceleration experiment presented is given.

3 Spectral Shape

At first an experimental setting, typical for TNSA was applied: A laser pulse with a ns-contrast ratio of 5×10^{-7} was obliquely ($45°$) incident on a Ti-foil target and the ions were detected in the target normal directions (front and rear). Typical ion spectra obtained with this setting are shown in Fig. 1(a), exhibiting strong asymmetry in energy and number of accelerated protons. The hot electrons exited at the front side traverse the target. After they have left the target at the rear side they propagate up to the Debye-length, where they are forced to turn around due to restoring electric field raised by the ions and re-enter the foil [3]. The blow-off plasma at the laser irradiated front side causes a flattened density gradient and therefore disintegration of the accelerating sheath field as expected [19, 20]. The subsequent plasma dynamic is described by an isothermal expansion of a quasi-neutral plasma on a time scale in the order of the laser pulse duration [21].

This situation changed drastically when the same experiment was repeated with UHC laser pulses achieved by the DPM. Here, the contrast is high enough to avoid a deterioration of the front side sheath field. The electrons re-circulate between the two Debye layers [22]. The bunch length L of the primarily accelerated electrons is approximated with $L = c\tau \approx 12\,\mu$m, where τ is the laser pulse duration and c the speed of light. Since this is on the order of twice the initial target thickness, the longitudinal electron distribution is confined by the target thickness D and twice the Debye length λ_D. In contrast to TNSA, the number of electrons permanently outside the foil Q becomes inversely proportional to the target thickness:

$$Q_{TNSA} = \frac{2N_e\lambda_D}{L} < \frac{2N_e\lambda_D}{D + 2\lambda_D} \quad \text{for:} \quad D < L/3, \tag{1}$$

where N_e electrons were initially accelerated by the laser. Secondly, in case of an UHC, the isothermal description of the plasma expansion is not well fitted anymore, since the main stage of ion acceleration in the expanding

plasma begins after the end of the laser pulse. A more suitable description of an adiabatic expansion was found to account for this [16, 23, 24]. The ion acceleration in a thin target continues after the end of the laser pulse almost symmetrically from both sides of the foil and drops down after the adiabatic cooling of fast electrons. A feature which was observed exactly as expected by theory (Fig. 1(b)) and which has been observed in another experiment [25]. It has to be denoted that the maximum ion energy obtained in this this regime equals the maximum energy of the TNSA regime but with half the laser intensity owing to the DPM efficiency. The dependence of the rising electron density by reducing the target thickness according to Eq. 1 has been exploited in several experiments leading to an optimum target thickness of around hundred nanometers [16, 20, 25]. This is also the reason why the ion energies are not enhanced even though the target thickness was decreased to 5 nm (Fig. 1(c)). But if the incidence of the laser was additionally changed to target normal, instead of 45° the maximum proton energy suddenly increased by a factor of three whereas the intensity was only increased by a factor of $\sqrt{2}$ due to the target rotation. This significant increase is related to the advanced phase matching of the accelerating electrons and the ions: The generation of hot electrons is partly suppressed due to the ultra-high contrast of the laser pulse and the normal incidence, i. e. the absence of the laser absorption processes Brunel- [26] and Resonance absorption.

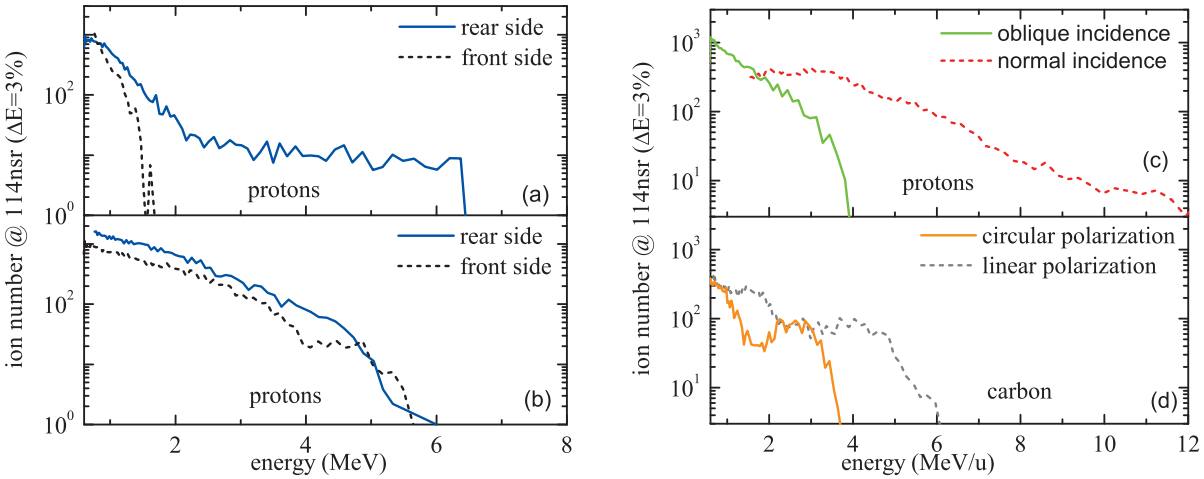

Fig. 1 (a) Protons from a Ti-5 μm foil with a contrast ratio of 10^{-7} and oblique incidence, (b) Protons from a Ti-5μm foil, UHC and oblique incidence, (c) protons from 5 nm DLC and UHC with oblique and normal incidence. In (d) the change of the spectral shape of the carbon (C^{6+}) ions is shown when the laser polarization is changed from linear to circular and UHC and normal incidence. (Online colour: www.cpp-journal.org).

The trapping of electrons at rest in the accelerating structure of the laser field can be obtained much easier due to their low mass compared to ions. The trapping velocity width [27] is $\sqrt{e\Phi/m_e} \sim c$, where Φ is the ponderomotive potential and m_e the electron mass. The ponderomotive potential is capable of inducing a wakefield with an amplitude $E \sim m_e\omega_p c/e$ and a velocity $\sim c$ which can still trap stationary electrons ("self-injection") [28]. The trapping velocity width of ions is much smaller than that of the electrons [5]:

$$v_{i,tr} \sim c\sqrt{\frac{m_e}{m_i}a_0 Q}, \tag{2}$$

where m_i and Q are the ion mass and charge. Since lasers with a normalized amplitude on the order of m_i/m_e are not available, the velocity of the accelerating structure has be reduced to be within $v_{i,tr}$. To accomplish these requirements, at first a transparent target has to be applied to provide an interaction region that extends throughout the whole focal volume and beyond. Secondly, the density of the target has to be adapted to the laser intensity [29] such that the group velocity of the laser field matches the ion trapping velocity. The transmittance determined experimentally (cf. section 4) is consistent with the analytical formula [1]:

$$T \cong 1/[1 + (\pi\sigma/\gamma_p)^2], \tag{3}$$

where γ_p is the peak Lorentz factor of the laser $\sqrt{a_L^2 + 1}$ and σ normalized areal electron density $\sigma = (n_e/n_c) \cdot (D/\lambda)$ [30]. n_e/n_c is the ratio of the electron- and the critical density, D the target thickness and λ the laser

wavelength. In case of a DLC foil with thickness 5 nm, the transmittance was $\sim 20\%$. And since the density is consistent with the empirical relation [29] $\sigma \approx 3 + 0.4 \times a_0 = 5$, the observed increase of the maximum proton energy (Fig. 1(c)) suggests the experimental demonstration of CAIL [5].

More specifically CAIL leads to RPA if circular laser polarization is used in the experiment. In this case, the generation of hot electrons can be further suppressed since the longitudinally oscillating component of the Lorentz force vanishes and Brunel- and resonance absorption are still disbanded due to the normal incidence of the laser pulse. In fact, the so-called RPA-concept [6, 12] consists of two stages: The initial stage, where the electrons are piled up to an equilibrium since the target ions are still immobile in that early stage and create a restoring electrical field. Later, the ions are set into motion layer-by-layer. And the light sail stage, where the target ions begin to move ballistically due to the electrical field created by the displaced and compressed electron layer which acts as an accelerated plasma mirror. During a few laser pulse cycles, a quasi-stationary state is established and the plasma cloud is accelerated with its center of mass moving at an almost constant velocity. The resulting ion spectra are intrinsically monoenergetic and an ion energy of 1 GeV can be theoretically obtained with a laser intensity of $\sim 10^{22}$ W/cm^2 [8].

The optimum condition for the RPA mechanism arises from the balance condition of the radiation pressure exerted on the electrons and the restoring electric field of the ions [8, 10] and is $a_0 \approx \sigma$, wich is fulfilled for a DLC target with a thickness of 5 nm under our experimental conditions: $5/\sqrt{2} = a_0 \approx \sigma = 3.3$. At this optimum condition the electron are not expelled totally from the ion and hence, only the ions in the electrons depletion layer will expand in a Coulomb explosion like manner, but are neglectable in terms of number and energy [31]. Whereas the onset of a peak-like structure was already visible if linear polarization was used, a distinct peak in the carbon spectrum is seen, centered around 30 MeV if the polarization is changed to circular (Fig. 1(d)). The shift of the peaks position from 4 MeV/amu to 2.8 Mev/amu is related to the decrease of the laser peak intensity by a factor of two when the laser polarization is changed from linear to circular. Two-dimensional particle-in-cell simulations revealed that those carbon ions are dominantly accelerated by the laser radiation pressure [15].

4 Optical Properties

Since the partial transmission of the intense laser pulse through an expanding target plays a decisive role to determine the dominant regime of ion acceleration [32–34], the opaqueness of the used foils is examined.

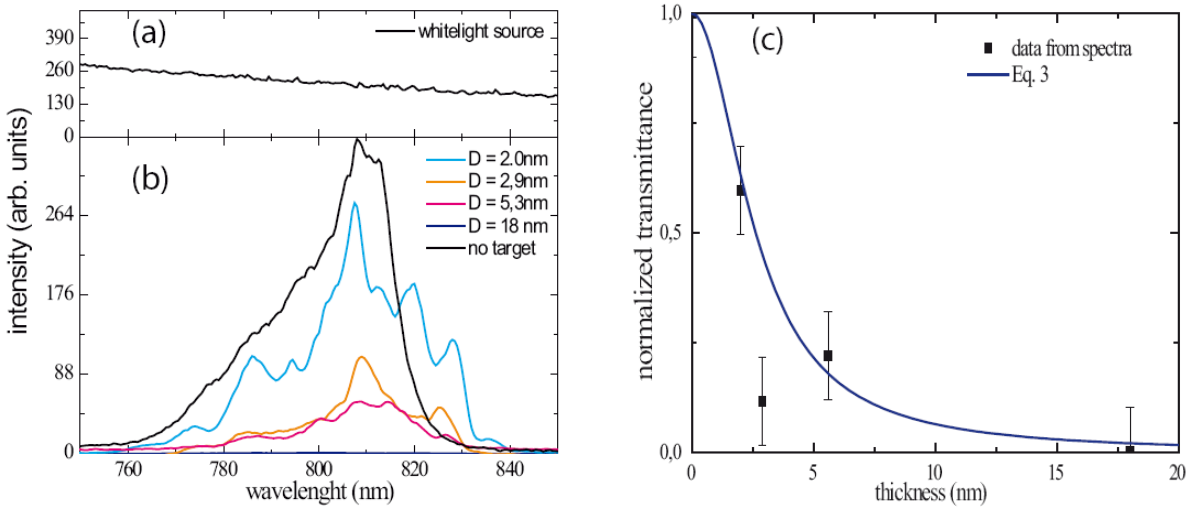

Fig. 2 (a) shows the signal of a constant white light source used for calibration of the optical path. (b) Measured, calibrated laser pulse spectra in transmittance of the DLC foils. (c) The resulting transmittance ($a_0 = 5$) of the DLC targets as a function of the target thickness obtained by numerical integrating the spectra of (b), compared to the analytical formula Eq. 3 from [1]. The errorbars are given by the average shot-to-shot fluctuation. (Online colour: www.cpp-journal.org).

For the experiments presented in this section, the target rear side was imaged to an optical grating spectrometer with 12-bit readout to (i) measure the transmittance of the laser pulse through the foil and (ii) obtain the spectral

properties of this nonlinear process. For calibration of the optical path and the spectrometer a commercial white light source delivering a constant intensity over a significant spectral range was introduced in the setup. In Fig. 2a the white light spectrum is shown which was used for calibrating the spectra shown in Fig. 2b.

Finally these calibrated spectra were numerically integrated to obtain the transmittance of the foils. To have an absolute measure of the transmittance, the shots were normalized to a shot without target. The experimental results for the transmission T are plotted along with the values expected by the analytical formula (Eq. 3).

To decrease the target thickness below 2.9 nm, where the electrons are expected to leave the electrostatic potential exerted by the ions [35], i. e. $a_0 > \sigma$ they were heated by a cw-laser with a power in the range of $100 - 500$ mW for several seconds, resulting in foil temperatures of $1000 - 3000$ K. Thereby it is assured that the water and hydrocarbon contamination layer is completely removed from the DLC foils. In fact, the ion spectra measured from these targets do not show any protons. Since the thickness of the contamination layer was determined to ~ 1 nm, the obtainable minimum thickness was ~ 2 nm.

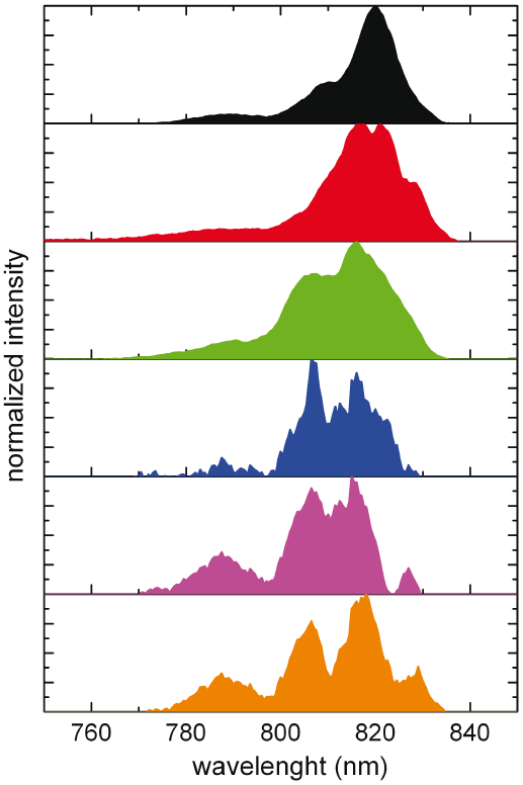

Fig. 3 Measured, calibrated laser pulse spectra in transmittance of the DLC foils with $\approx$ 2nm thickness revealing strong spectral modulation and broadening. (Online colour: www.cpp-journal.org).

The situation changes drastically again when these pre-heated targets were used in the experiment. The targets are getting highly transparent and the spectrum (Fig. 2b) exhibits a strong modulation and is broadened significantly. To have a closer look at this feature, in Fig. 3 several spectra, obtained for a thickness of ~ 2 nm are plotted. They demonstrate the whole bandwidth of the modulation and broadening at this thickness. The spectral broadening potentially gives rise to the onset of pulse-shortening due to the non-linear interaction: The transmittance Eq. 3 is a function of the laser amplitude a_0 and hence of the intensity. Thus, a small fraction associated with the most intense part of the laser pulse is transmitted, the rest reflected or absorbed. The transmitted pulse can therefore be much shorter than the incident pulse [36].

5 Conclusion

In conclusion we sketched the route towards the current optimum of laser generated ion beams by subsequently changing the important parameters such as target thickness, laser pulse contrast, angle of incidence and laser pulse polarization. Beginning with parameters of isothermal TNSA, we reached the regime where the plasma expansion can be described adiabatically and results in a symmetric ion acceleration. Further we demonstrated

a way to phase match the accelerating electron population with the ions, namely CAIL, which finally leads to RPA. While the maximum energy and the ion number were obtained with linear polarization of the laser pulse, the most promising acceleration scenario, with respect to the scalability of the ion energy with the laser intensity, RPA was reached using circularly polarized laser pulses.

Furthermore, the opaqueness of the foils was examined. Here, the measured transmission is in good agreement with the values calculated analytically [30]. The spectral shape of the transmitted light includes strong modulations and exhibits a significant spectral broadening. A further influence of the temporal pulse shape is initiated that could lead to the generation of ultra-short transmitted pulses [36] and therefore suggests the use of double targets [37].

Acknowledgements This work was supported by Deutsche Forschungsgemeinschaft through Transregio SFB TR18 and the DFG-Cluster of Excellence Munich-Centre for Advanced Photonics (MAP). A. A. A. acknowledges financial support from EU Grant (Marie Curie) (No. PIIF-GA-2008-221727) and P. V. N. from the WCU department of GIST.

References

[1] S. Steinke, A. Henig, M. Schnuerer, T. Sokollik, P. V. Nickles, D. Jung, D. Kiefer, R. Hoerlein, J. Schreiber, T. Tajima, X. Q. Yan, M. Hegelich, J. Meyer ter Vehn, W. Sandner, and D. Habs, Laser and Particle Beams **28**, 215 (2010).
[2] S. C. Wilks, A. B. Langdon, T. E. Cowan, M. Roth, M. Singh, S. Hatchett, M. H. Key, D. Pennington, A. MacKinnon, and R. A. Snavely, Physics of Plasmas **8**, 542 (2001).
[3] J. Schreiber, F. Bell, F. Gruener, U. Schramm, M. Geissler, M. Schnuerer, S. Ter-Avetisyan, B. M. Hegelich, J. Cobble, E. Brambrink, J. Fuchs, P. Audebert, and D. Habs, Physical Review Letters **97**, 045005 (2006).
[4] X. Q. Yan, T. Tajima, M. Hegelich, L. Yin, and D. Habs, Applied Physics B: Lasers and Optics **98** (2009).
[5] T. Tajima, D. Habs, and X. Q. Yan, Reviews of Accelerator Science and Technology **2**, 201 (2009).
[6] A. Macchi, F. Cattani, T. V. Liseykina, and F. Cornolti, Physical Review Letters **94**, 165003 (2005).
[7] X. Zhang, B. Shen, X. Li, Z. Jin, and F. Wang, Physics of Plasmas **14**, 073101 (2007).
[8] O. Klimo, J. Psikal, J. Limpouch, and V. T. Tikhonchuk, Physical Review Special Topics-Accelerators and Beams **11**, 031301 (2008).
[9] A. P. L. Robinson, M. Zepf, S. Kar, R. G. Evans, and C. Bellei, New Journal of Physics **10**, 013021 (2008).
[10] X. Q. Yan, C. Lin, Z. M. Sheng, Z. Y. Guo, B. C. Liu, Y. R. Lu, J. X. Fang, and J. E. Chen, Physical Review Letters **100**, 135003 (2008).
[11] B. Qiao, M. Zepf, M. Borghesi, and M. Geissler, Physical Review Letters **102**, 145002 (2009).
[12] A. Macchi, S. Veghini, T. V. Liseykina, and F. Pegoraro, New Journal of Physics **12**, 045013 (2010).
[13] B. Qiao, M. Zepf, M. Borghesi, B. Dromey, M. Geissler, A. Karmakar, and P. Gibbon, Physical Review Letters **105**, 155002 (2010).
[14] T. P. Yu, A. Pukhov, G. Shvets, and M. Chen, Physical Review Letters **105**, 065002 (2010).
[15] A. Henig, S. Steinke, M. Schnuerer, T. Sokollik, R. Hoerlein, D. Kiefer, D. Jung, J. Schreiber, B. M. Hegelich, X. Q. Yan, J. Meyer ter Vehn, T. Tajima, P. V. Nickles, W. Sandner, and D. Habs, Physical Review Letters **103**, 245003 (2009).
[16] A. A. Andreev, S. Steinke, T. Sokollik, M. Schnurer, S. Ter Avetsiyan, K. Y. Platonov, and P. V. Nickles, Physics of Plasmas **16**, 013103 (2009).
[17] A. Lévy, T. Ceccotti, P. D'Oliveira, F. Reau, M. Perdrix, F. Quere, P. Monot, M. Bougeard, H. Lagadec, P. Martin, J. P. Geindre, and P. Audebert, Optics Letters **32**, 310 (2007).
[18] S. Ter-Avetisyan, M. Schnuerer, and P. V. Nickles, Journal of Physics D-Applied Physics **38**, 863 (2005).
[19] M. Kaluza, J. Schreiber, M. I. K. Santala, G. D. Tsakiris, K. Eidmann, J. Meyer ter Vehn, and K. J. Witte, Physical Review Letters **93**, 045003 (2004).
[20] D. Neely, P. Foster, A. Robinson, F. Lindau, O. Lundh, A. Persson, C. G. Wahlstrom, and P. McKenna, Applied Physics Letters **89**, 021502 (2006).
[21] P. Mora, Physical Review Letters **90**, 185002 (2003).
[22] Y. Sentoku, T. E. Cowan, A. Kemp, and H. Ruhl, Physics of Plasmas **10**, 2009 (2003).
[23] M. Murakami and M. M. Basko, Physics of Plasmas **13**, 012105 (2006).
[24] A. A. Andreev, A. Lévy, T. Ceccotti, C. Thaury, K. Platonov, R. A. Loch, and P. Martin, Physical Review Letters **101**, 155002 (2008).
[25] T. Ceccotti, A. Levy, H. Popescu, F. Reau, P. D'Oliveira, P. Monot, J. P. Geindre, E. Lefebvre, and P. Martin, Physical Review Letters **99**, 185002 (2007).
[26] F. Brunel, Physical Review Letters **59**, 52 (1987).
[27] E. Esarey and M. Pilloff, Physics of Plasmas **2**, 1432 (1995).

[28] W. P. Leemans, C. W. Siders, E. Esarey, N. E. Andreev, G. Shvets, and W. B. Mori, Ieee Transactions on Plasma Science **24**, 331 (1996).
[29] T. Esirkepov, M. Yamagiwa, and T. Tajima, Physical Review Letters **96**, 105001 (2006).
[30] V. A. Vshivkov, N. M. Naumova, F. Pegoraro, and S. V. Bulanov, Physics of Plasmas **5**, 2727 (1998).
[31] A. A. Andreev, S. Steinke, M. Schnuerer, A. Henig, P. V. Nickles, K. Y. Platonov, T. Sokollik, and W. Sandner, Physics of Plasmas **17**, 123111 (2010).
[32] E. d'Humieres, E. Lefebvre, L. Gremillet, and V. Malka, Physics of Plasmas **12**, 062704 (2005).
[33] L. Yin, B. J. Albright, B. M. Hegelich, and J. C. Fernandez, Laser and Particle Beams **24**, 291 (2006).
[34] B. J. Albright, L. Yin, K. J. Bowers, B. M. Hegelich, K. A. Flippo, T. J. T. Kwan, and J. C. Fernandez, Physics of Plasmas **14**, 094502 (2007).
[35] D. Kiefer, A. Henig, D. Jung, D. C. Gautier, K. A. Flippo, S. A. Gaillard, S. Letzring, R. P. Johnson, R. C. Shah, T. Shimada, J. C. Fernández, V. K. Liechtenstein, J. Schreiber, B. M. Hegelich, and D. Habs, The European Physical Journal D - Atomic, Molecular, Optical and Plasma Physics **55**, 427 (2009).
[36] L. L. Ji, B. F. Shen, X. M. Zhang, F. C. Wang, Z. Y. Jin, C. Q. Xia, M. Wen, W. P. Wang, J. C. Xu, and M. Y. Yu, Physical Review Letters **103**, 215005 (2009).
[37] T. Kluge, W. Enghardt, S. D. Kraft, U. Schramm, Y. Sentoku, K. Zeil, T. E. Cowan, R. Sauerbrey, and M. Bussmann, Physical Review E **82**, 016405 (2010).

